



Esterification of Sesbania Gum Hydrolysate in Ionic Liquid, Optimization and Characterization of Its Derivatives

Hongbo Tang¹ · Pingxiu Sun¹ · Yanping Li¹ · Siqing Dong¹

Received: 16 January 2019 / Accepted: 1 April 2019 / Published online: 16 April 2019
© King Fahd University of Petroleum & Minerals 2019

Abstract

The goal of this work focuses to optimize some parameters in esterification process of sesbania gum hydrolysate by response surface methodology, and to characterize sesbania gum and its derivatives. The experimental results indicated that degree of substitution (DS) of maleate enzymolysis sesbania gum (MESG) could reach a value of 0.768 when an ionic liquid, that is, 1-butyl-3-methylimidazolium chloride, was used as a solvent during the esterification. The obtained regression model could well evaluate the synthesis of MESG. The stretching vibration peak of C–H bonds in MESG was split into two peaks at the wave numbers of 3937 and 2886 cm^{-1} owing to high DS. The esterification almost changed the crystalline structure of MESG into an amorphous one, whereas the enzymatic hydrolysis less affected the crystalline structure of sesbania gum (SG). The structure of SG granules was severely destroyed by such an esterification with an ionic liquid. The esterification increased the thermal stability of SG. Adding MESG could obviously influence the potato starch pasting characteristics such as peak viscosity, trough viscosity, final viscosity, setback and breakdown.

Keywords Sesbania gum · Enzymolysis · Esterification · Ionic liquid · Optimization

1 Introduction

Sesbania gum (SG) is a kind of natural semi-galactose macromolecular compound obtained by mechanical or chemical treatment [1, 2], and its composition is consistent with that of guar gum [3, 4]. The molecular structure of SG indicates that each monosaccharide of SG chains includes three hydroxyl groups, which can be etherified, esterified, oxidized and so on [5]. Due to the presence of hydroxyl groups, SG has a strong affinity for water and forms a gel by cross-linking

with water. SG is widely used in petroleum, paper, textile, medicine, food, mining, printing and dyeing because of its very good adhesion, flocculation and flotation performances at low concentration [6, 7]. However, the shortcomings of SG such as slow hydration, high water-insoluble content and poor shear resistance make its application to be very limited [8]. Therefore, SG needs to be modified to meet the requirements of the practical applications. The esterification is one of the most commonly used chemical modifications for natural polymers, for example, starch, guar gum, cellulose and so on [9–11], and it is able to improve the properties of these natural polymers, including film forming [12], emulsifying [13], hydrophilicity [14], gelation [15], etc. At present, the used esterifications for the modification of natural polymers include wet [16, 17], semi-dry [18] and dry methods [19, 20]. The organic solvent method and ionic liquid method, which are often used to prepare the derivatives of natural polymers with high substitution degree, belong to the wet method. Owing to the toxicity and post-treatment problems of organic solvent method, however, its overall effect will be worse than that of ionic liquid method in the aspect of stability and environmental friendliness [21]. At present, the modifications of SG include phosphorylation [22], oxidization [23], graft [24], carboxymethylation [25, 26], cross-linking [27]

✉ Hongbo Tang
tanghb6666@sina.com

Pingxiu Sun
spx6306@163.com

Yanping Li
lypsut@163.com

Siqing Dong
dongsiqing6666@sina.com

¹ Science School, Shenyang University of Technology, No. 111 Shenliao West Road Economic & Technological Development Zone, Shenyang City 110870, People's Republic of China



and so on, whereas its esterification of maleic anhydride is not found so far.

In this work, SG was modified using a combination of enzymolysis with esterification for the first time, and degree of substitution (DS) of maleate enzymolysis sesbania gum (MESG) could reach a value of 0.768, which was different from the traditional methods. Therefore, β -1,4-D-mannanase was selected to hydrolyze SG to provide products with short chains and low viscosity for further modification, and an ionic liquid was chosen as a solvent to increase the substitution degree of MESG and the esterification efficiency. On basis of this, we further investigated the effect of esterification and enzymatic hydrolysis on the structure and properties of SG by means of infrared spectrometer, X-ray diffractometer, thermogravimetric analyzer, scanning electron microscope and so on. As a result, the esterification will provide a reliable option for introducing the novel and functional groups into SG molecular chains.

2 Materials and Methods

2.1 Materials

Sesbania gum (SG) was purchased from Xiangshui Unified Guar Gum Co. Ltd. Potato starch was purchased from Ningxia Guyuan Longxin Starch Co.Ltd. β -1, 4-D-mannan manno-hydrolase was purchased from Sinopharm Chemical Reagent Shenyang Co. Ltd. Maleic anhydride was purchased from Tianjin Ruijinte Chemical Co., Ltd. 1-Butyl-3-methylimidazolium chloride (ionic liquid, BMIMCl) was purchased from CAS Lanzhou Institute of Chemical Physics (China). The other reagents include pyridine, hydrochloric acid, anhydrous glucose, sodium hydroxide, ethanol and phenolphthalein, and are analytic grade.

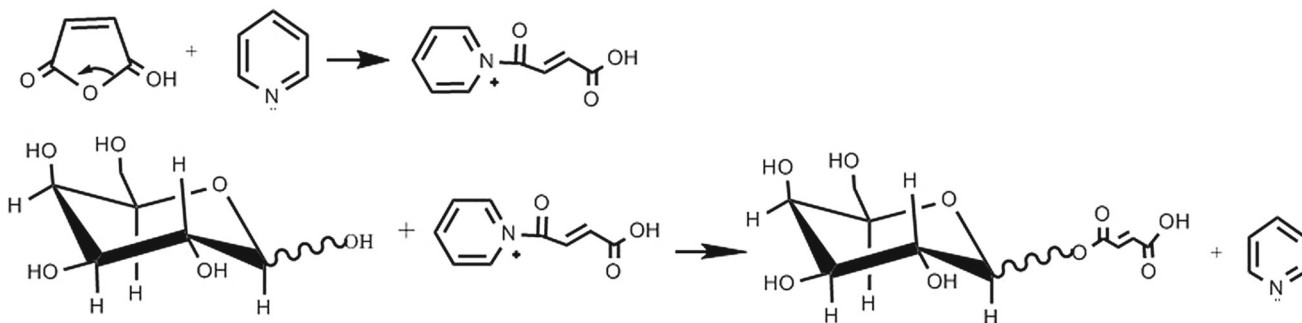
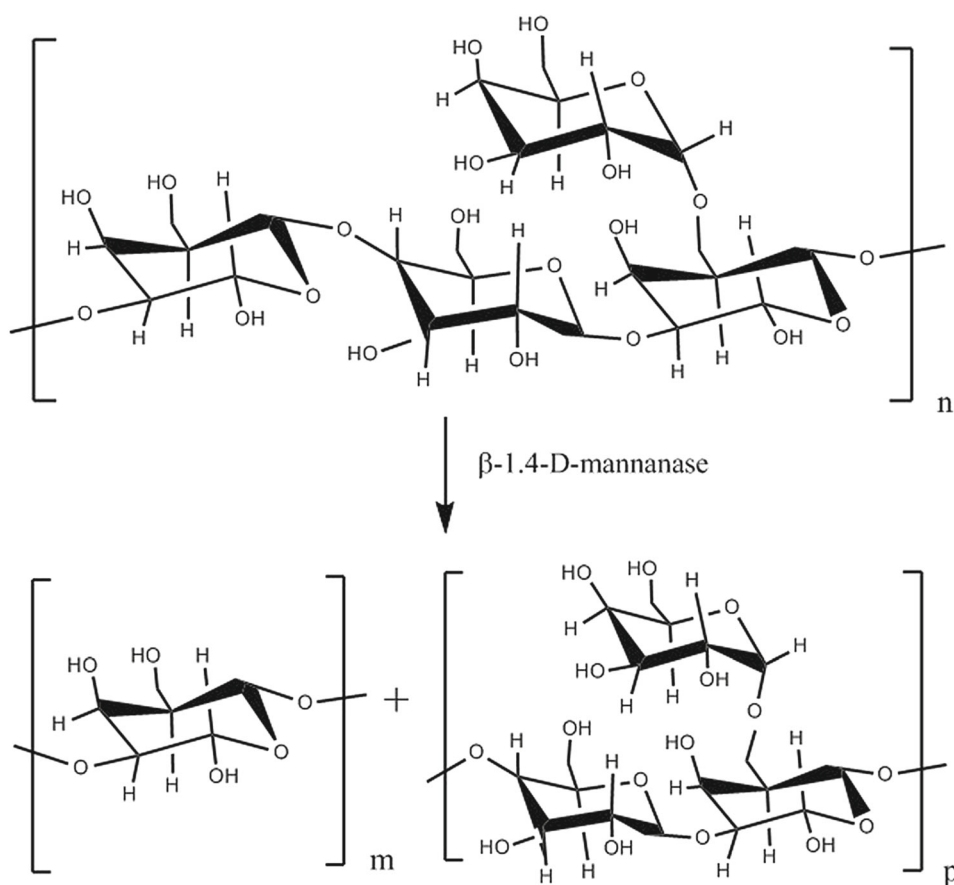
2.2 Preparation of Enzymolysis Sesbania Gum (ESG) and Maleate Enzymolysis Sesbania Gum (MESG)

A total of 10.0 g of SG (dry) is mixed with ethanol solutions with a mass concentration of 30% (w/w, the same below) in a 250-mL three-necked flask equipped with stirrer to prepare a suspension with a concentration of 10% and stirred, heating it to the temperature of 65 °C in a water bath and then adding 200 u/g of β -1,4-D-mannan manno-hydrolase. After the enzymolysis for 8 h, the pH of mixture was adjusted to 2 with 10% of hydrochloric acid solution and kept for 15 min to rapidly inactivate the enzyme, and then the pH was adjusted back to 7 with 5% of sodium hydroxide solution. The mixture was filtrated by a Buchner funnel filter, and the obtained cake was washed for 3–4 times with ethanol solutions with a mass concentration of 60%, dried, pulverized and sieved. Finally, ESG was obtained [28].

A total of 70.0 g of ionic liquid was placed into a 250-mL three-necked flask and heated to 115 °C in an oil bath until it was completely melted, and then 5.0 g of ESG (dry) was added and the mixture fully stirred. After that, we added 4 g of maleic anhydride, made the system to reflux for 5 min and then slowly added dropwise 1.5 mL of pyridine through a constant pressure funnel within 15 min. After the reaction for 80 min, 200 mL of ethyl alcohol with temperature of 50 °C was poured into the mixture grinded and then filtered. After mixing the obtained cake with the appropriate amount of ethanol with a concentration of 95%, it was grinded and filtered. The above washing operations were repeated for three times again. Afterward, the resulting cake was immersed into appropriate amount of ethanol with a concentration of 95% and rested for 24 h until the product was completely separated from the ionic liquid. Finally, the suspension was filtered again, and the obtained filter cake was dried under an infrared lamp and then pulverized and sieved to obtain

MESG powders [29]. The schematic diagram of enzymolysis and etherification was as follows:

(glucose). The higher the DE value, the greater the hydrolysis degree of SG was. The DE value was calculated as follows:



2.3 Determination of Enzymatic Hydrolysis Degree and Degree of Substitution (DS)

The enzymolysis degree of SG was evaluated by DE value, and DE value was determined by a DNS method [30]. The value of DE was referred to as the content of reducing sugar

$$DE(\%) = \frac{\text{Reducing sugar (expressed by glucose)}}{\text{Sample mass (dry)}} \times 100 \tag{1}$$

The substitution degree of MESG was determined by a method reported by the literature, that is, an acid–base titra-

tion [31]. The degree of substitution (DS) of samples was calculated by the following equation.

$$W_{\text{MLA}} = \frac{98C(V_0 - V)}{1000 \times 2W} \times 100\% \quad (2)$$

$$\text{DS} = \frac{162W_{\text{MLA}}}{98 \times (100 - W_{\text{MLA}})} \quad (3)$$

where W_{MLA} is the content of maleic anhydride substituted, %; W is the mass of sample, g; C is the concentration of HCl solution, mol/L; V_0 is the volume of HCl solution consumed by blank, mL; and V is the volume of HCl solution consumed by sample, mL.

2.4 Fourier Transform Infrared Spectroscopy (FTIR), X-Ray Diffraction (XRD), Particle Morphology and Thermal Analysis

The crystalline structure of SG and modified SG was analyzed by an X'Pert Pro MPD X-ray diffractometer (PANalytical Co., Ltd., the Netherlands) [32]. We used an IR Prestige-21 infrared spectrometer (Shimadzu Corporation, Japan) to record FTIR spectra within the 4000–400 cm^{-1} range and in a solid state using the KB pellet method [33, 34]. The particle morphology was obtained by a Phenom ProX SEM equipped with spectrometer (Shanghai Feina Scientific Instruments Company Limited, China) [35]. The thermal analysis of SG or its derivatives was carried out with a TGA Q50 V20.10 Build 36 thermogravimetric analyzer and a DSC Q20 V24.4 Build 116 differential scanning calorimeter (TA Instruments, US) in a nitrogen atmosphere [36, 37].

2.5 Pasting Behavior of Starch Containing SG or Its Derivatives

A total of 5 g of dry potato starch evenly mixed with 0.015 g of dry SG or its derivatives was placed into a 100-mL beaker with 96 mL distilled water. After SG or its derivatives being dissolved thoroughly, about 25 mL of the suspension was taken out and slowly poured into the cylinder. Pasting behavior of starch was determined by a MCR102 rheometer (Anton Paar, Austria). Pasting conditions were temperature range 50–95 °C, heating and cooling rate 6.0 °C/min, rotation rate of agitator 960 rpm for first 10 s, and 160 rpm for other time [38].

2.6 Experimental Design of Response Surface Test

The Design-Expert software 8.05b was used for designing the statistical test, analyzing the results and drawing the response surface plots. The second-degree polynomial model was chosen to assess the relationships between independent variables and dependent variable. On basis of single-factor test, the

response surface test was designed by selecting the reaction temperature, amount of maleic anhydride, reaction time and amount of ionic liquid as independent variables, and DS was chosen as a response value to optimize the process conditions of preparing MESH. The actual values of the factors were varied at three levels, namely – 1, 0 and + 1 corresponding to minimum, middle and maximum. The factors and coded levels of Box–Behnken test are listed in Table 1.

3 Results and Discussion

3.1 Effect of Reaction Temperature, Reaction Time, Amount of Pyridine, Amount of Maleic Anhydride and Ionic Liquid on DS of MESH

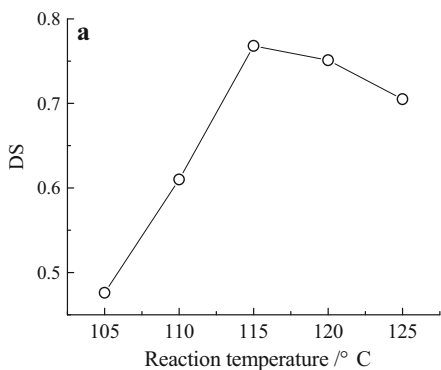
The effect of the reaction temperature, reaction time, amount of pyridine, amount of maleic anhydride and ionic liquid on DS of MESH is shown in Fig. 1. The range of reaction temperature was chosen from 105 to 125 °C to investigate the effect of the reaction temperature on DS of MESH, and the range of reaction time was from 40 min to 120 min, amount of pyridine from 10 to 50%, amount of maleic anhydride from 20 to 60% and amount of ionic liquid from 1000 to 1800%. Here, the amount of pyridine, the amount of maleic anhydride and the amount of ionic liquid were, respectively, defined as the percentage ratio of pyridine, maleic anhydride and ionic liquid to dry ESG.

From Fig. 1, the variation tendency of the reaction temperature influencing on DS of MESH was same as that of maleic anhydride amount, that is, the variation of both in DS of MESH first increased and then decreased, and there was a maximum DS of the obtained MESH. The effect of reaction time on DS of MESH was similar to the effect of ionic liquid amount on DS of MESH. When the reaction time was above 80 min, the slight decrease in DS of MESH might be the result of the deesterification in the alkaline environment. Before the amount of ionic liquid reached the necessary value, it greatly influenced on DS. So the necessary amount of ionic liquid should be provided to ensure the effective esterification. The effect of amount of maleic anhydride on DS of MESH was also different from other esterification, that is, DS of MESH did not rise as increasing the amount of maleic anhydride. The small DS value at low temperature should be a result of ionic liquids not dissolving more ESG at that temperature. The slight reduction in DS at high temperature might come from the increase in the side reaction. Pyridine as a catalyst was added during the esterification and evidently influenced the reaction. From Fig. 1d, the suitable amount of pyridine could be beneficial to the esterification, whereas the high amount of pyridine contributed small to the esterification. When the amount of pyridine was 20%, DS of MESH could reach a value of 0.684, indicating that the amount of pyridine

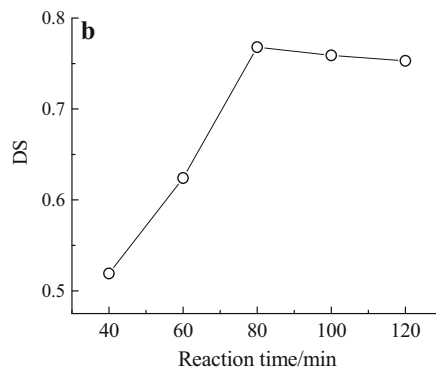
Table 1 Factors and levels of MESG response surface test

Factor and level	Reaction temperature (A) (°C)	Amount of maleic anhydride (B) (%)	Amount of ionic liquid (C) (%)	Reaction time (D) (min)
- 1	110	30	1200	60
0	115	40	1400	80
1	120	50	1600	100

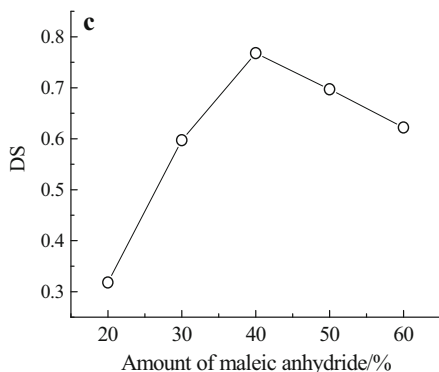
Fig. 1 Effect of reaction temperature (a), reaction time (b), amount of maleic anhydride (c), amount of pyridine (d) and amount of ionic liquid (e) on DS of MESG



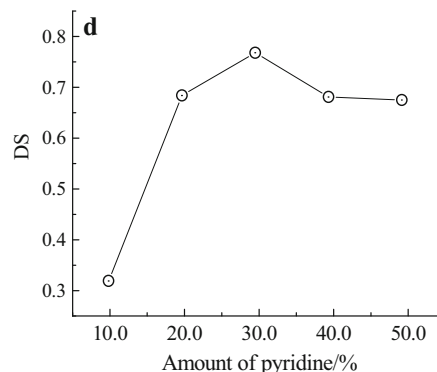
Reaction conditions: reaction time 80 min, amount of maleic anhydride 40%, amount of pyridine 30%, amount of ionic liquid 1400%.



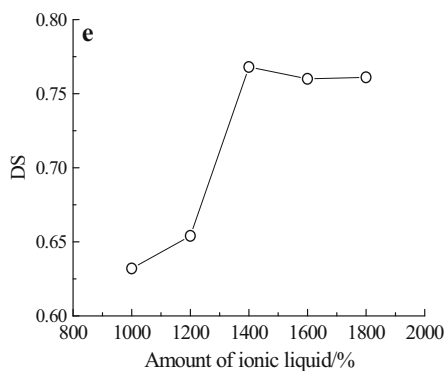
Reaction conditions: reaction temperature 115 °C, amount of maleic anhydride 40%, amount of pyridine 30 %, amount of ionic liquid 1400%.



Reaction conditions: reaction time 80 min, reaction temperature 115 °C, amount of pyridine 30%, amount of ionic liquid 1400%.



Reaction conditions: reaction time 80 min, reaction temperature 115 °C, amount of maleic anhydride 40%, amount of ionic liquid 1400%.



Reaction conditions: reaction time 80 min, reaction temperature 115 °C, amount of pyridine 30%, amount of maleic anhydride 40%.

Table 2 Design and result of MESH response surface test

Test numbers	A (°C)	B (%)	C (%)	D (min)	DS
1	0	-1	1	0	0.551
2	0	1	0	-1	0.812
3	-1	-1	0	0	0.587
4	1	0	0	1	0.685
5	0	0	0	0	0.730
6	1	-1	0	0	0.610
7	0	1	1	0	0.703
8	-1	0	-1	0	0.524
9	0	1	-1	0	0.629
10	0	0	0	0	0.768
11	1	0	-1	0	0.664
12	0	0	-1	1	0.603
13	0	0	0	0	0.726
14	0	-1	0	-1	0.529
15	0	-1	0	1	0.659
16	-1	0	1	0	0.597
17	-1	0	0	1	0.631
18	-1	0	0	-1	0.551
19	0	0	1	1	0.693
20	1	1	0	0	0.749
21	1	0	1	0	0.733
22	0	0	-1	-1	0.584
23	1	0	0	-1	0.672
24	-1	1	0	0	0.579
25	0	-1	-1	0	0.564
26	0	0	0	0	0.731
27	0	1	0	1	0.726
28	0	0	1	-1	0.642
29	0	0	0	0	0.768

was not less than 20%, which was able to ensure to obtain MESH with high DS.

Above all, the suitable reaction conditions were as follows: reaction temperature 115 °C, reaction time 80 min, amount of maleic anhydride 40%, amount of pyridine 30% and amount of ionic liquid 1400%.

3.2 Response Surface Optimization for Preparing MESH

The design and result of the response surface test are listed in Table 2. The amount of pyridine was held at 30%.

Based on experimental data in Table 2, the second-order response surface model for preparing MESH with high DS was obtained, that is,

$$DS = 0.74 + 0.054A + 0.058B + 0.029C + 0.017D + 0.037AB - 0.001AC - 0.017AD$$

$$+ 0.022BC - 0.054BD + 0.008CD - 0.061A^2 - 0.047B^2 - 0.073C^2 - 0.035D^2 \quad (4)$$

To check the significance of the above second-order polynomial equation, the variance analysis is done and listed in Table 3. From Table 3, it could be seen that the *F* value of the model was 11.76 and the *p* value of the model was less than 0.0001, indicating that the regression model was extremely significant, and the DS of MESH could be evaluated by using this model. In the analysis of variance, the *p* value of each item indicated the influence of the corresponding item on the level of DS. The items *A*, *B*, *C*, A^2 , B^2 , C^2 and *BD* were extremely significant ($p < 0.01$), the items *D*, *AB* and D^2 were significant ($p < 0.05$), while other items were not significant. Therefore, the final optimized equation was simplified as follows:

$$DS = 0.74 + 0.054A + 0.058B + 0.029C + 0.017D + 0.037AB - 0.054BD - 0.061A^2 - 0.047B^2 - 0.073C^2 - 0.035D^2 \quad (5)$$

According to the analysis of variance, the factors influencing the esterification of MESH from strong to weak were as follows: reaction temperature, amount of maleic anhydride, amount of ionic liquid and reaction time. The determination coefficient (*R*²) was 0.9142, implying that 91.42% of the variation could be explained by the regression model. Therefore, the model had a high credibility. According to the equation, the corresponding process conditions were optimized as follows: reaction time 79.64 min, reaction temperature 119.71 °C, amount of maleic anhydride 40.4% and amount of ionic liquid 1403%. Considering the feasibility of the practical operation, the optimum reaction conditions were adjusted to reaction time 80 min, reaction temperature 119 °C, amount of maleic anhydride 40% and amount of ionic liquid 1400%.

Known from the above analysis, since the interaction items *AB* and *BD* were extremely significant and significant, respectively, the response surfaces of the interaction items *AB* and *BD* are shown in Figs. 2 and 3. According to Figs. 2 and 3, the shape of the response surface of Fig. 2 was different from that of Fig. 3. The maximum DS value for the mutual effect between reaction temperature and amount of maleic anhydride was at suitable reaction temperature and amount of maleic anhydride, whereas maximum DS for the mutual effect between reaction time and amount of maleic anhydride appeared at the maximum amount of maleic anhydride and suitable reaction time.

Finally, in order to verify the reliability of the model, we made three parallel tests according to the optimal process parameters which had been determined. The result indicated that the average DS of MESH was 0.756, which was close to

Table 3 Variance analysis for influencing components in MESG response surface test

Source	Sum of square	Degree of freedom	Mean square	<i>F</i> value	<i>p</i> value
Model	0.16	14	5.265×10^{-3}	11.76	<0.0001
<i>A</i>	0.035	1	0.016	36.42	<0.0001
<i>B</i>	0.041	1	0.018	40.16	<0.0001
<i>C</i>	0.010	1	4.772×10^{-3}	10.66	0.0056
<i>D</i>	3.571×10^{-3}	1	2.163×10^{-3}	4.83	0.0453
<i>AB</i>	5.402×10^{-4}	1	2.262×10^{-3}	5.05	0.0413
<i>AC</i>	4.697×10^{-5}	1	4.697×10^{-5}	0.10	0.7508
<i>AD</i>	6.390×10^{-4}	1	6.390×10^{-4}	1.43	0.2521
<i>BC</i>	8.536×10^{-4}	1	8.536×10^{-4}	1.91	0.1890
<i>BD</i>	5.188×10^{-3}	1	5.188×10^{-4}	11.59	0.0043
<i>CD</i>	9.306×10^{-5}	1	9.306×10^{-3}	0.21	0.6555
<i>A</i> ²	0.010	1	0.010	22.76	0.0003
<i>B</i> ²	6.490×10^{-3}	1	6.490×10^{-3}	14.50	0.0019
<i>C</i> ²	0.015	1	0.015	32.59	<0.0001
<i>D</i> ²	3.394×10^{-3}	1	3.394×10^{-3}	7.58	0.0156
Residual	6.268×10^{-3}	14	4.477×10^{-4}		
Lack of fit	5.649×10^{-3}	10	5.649×10^{-4}		
Pure error	26.198×10^{-4}	4	1.550×10^{-4}		
Cor total	0.080	28			

$p < 0.05$, significant difference; $p < 0.01$, extremely significant difference

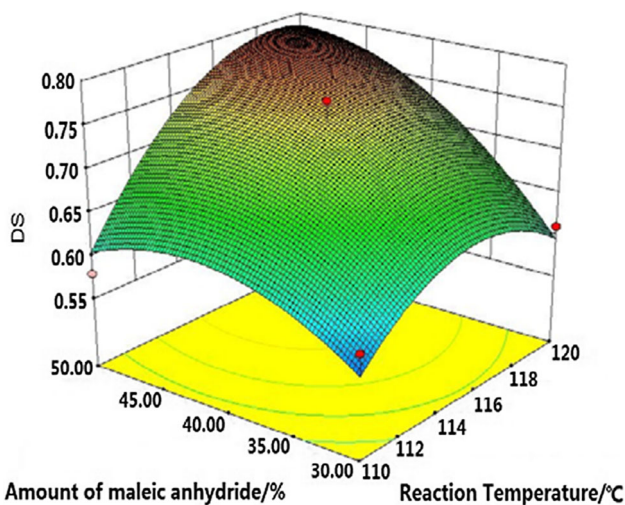


Fig. 2 Response surfaces of mutual effect between reaction temperature and amount of maleic anhydride at reaction time 80 min and amount of ionic liquid 1400%

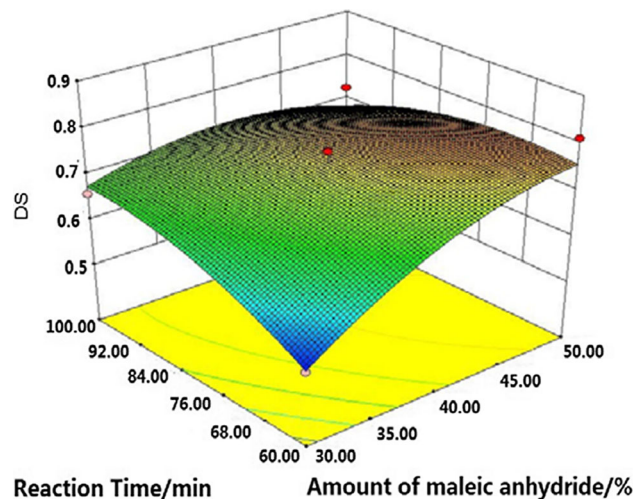


Fig. 3 Response surfaces of mutual effect between reaction time and amount of maleic anhydride at reaction temperature 119 °C and amount of ionic liquid 1400%

the value of 0.762 predicted by above model. It showed that the model was used to well predict DS of MESG.

3.3 FTIR Analysis

FTIR spectra of SG, ESG (DE = 0.175) and MESG (DE = 0.175, DS = 0.812) are shown in Fig. 4. From Fig. 4, the stretching vibration peaks of O–H groups of three samples

appeared at the wave numbers of 3405 cm^{-1} [39], but the peak intensity of hydroxyl groups of MESG was obviously less than that of SG and ESG, suggesting that the numbers of O–H groups in MESG were reduced due to introduction of ester groups. The stretching vibration peak of C–H bonds in MESG was also different from those of SG and ESG and was split into two peaks appearing separately at the wave numbers of 3937 and 2886 cm^{-1} . In MESG spectrum, a new

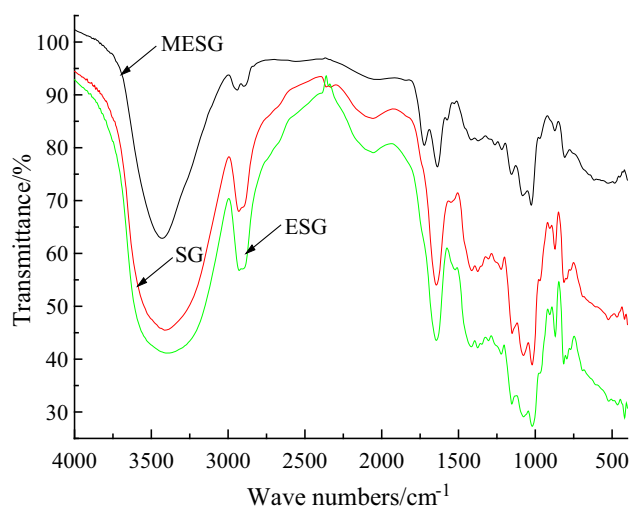


Fig. 4 FTIR spectra of SG, ESG and MESH

peak appeared very clearly at 1718 cm^{-1} and belonged to the stretching vibration of C=O groups, which was consistent with that in the literature [40]. It confirmed that ESG was already esterified in ionic liquid. The vibration peak of C–O–C bonds still appeared at 1151 cm^{-1} , indicating that C–O–C bonds were not influenced by the esterification.

3.4 Thermal Analysis

The TGA and DSC curves of SG, ESG (DE = 0.175) and MESH (DE = 0.175, DS = 0.812) are shown in Fig. 5. From Fig. 5, the TGA and DSC curves of MESH varied greatly, whereas TGA and DSC curves of ESG changed small, compared with those of SG. The esterification elevated the lower segment of the TGA curve of SG, moved the TGA curve of ESG to the left and reduced the intensity of the endothermic peak of MESH. It indicated that the esterification and enzymatic hydrolysis could influence the thermal properties of SG. To compare the effect of esterification and enzymatic hydrolysis on the thermal properties of SG, the corresponding key characteristic parameters about these

Fig. 5 TGA (left), DSC (right) curves of SG, ESG and MESH

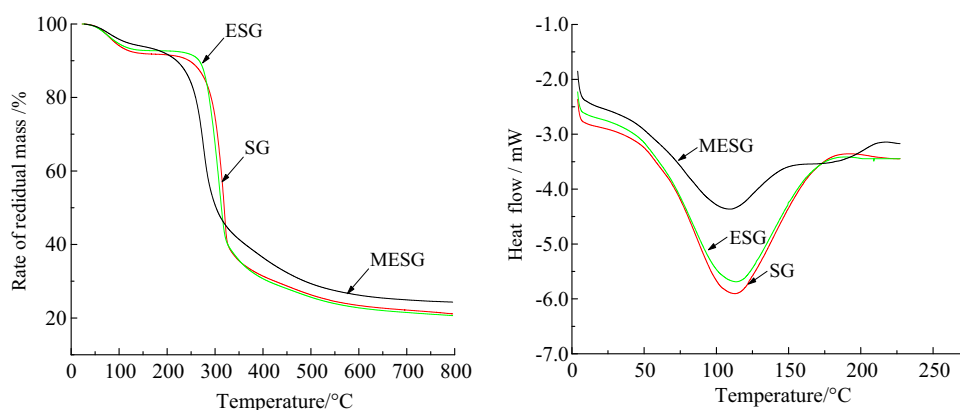


Table 4 The TGA, DSC thermodynamics data of SG, ESG and MESH

Samples	SG	ESG	MESH
Onset decomposition temperature (°C)	288.0	278.8	253.2
End decomposition temperature (°C)	331.6	328.8	306.0
Weight loss rate (%)	43.2	46.7	34.0
Onset temperature (°C)	56.9	52.5	44.8
Peak temperature (°C)	111.9	112.4	107.6
End temperature (°C)	169.3	166.9	212.7
Enthalpy change (J g^{-1})	287.4	242.0	227.9

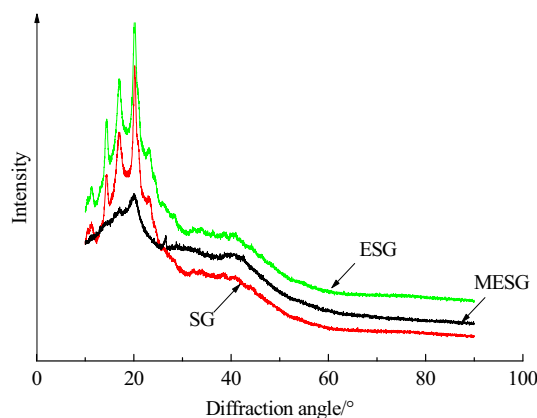
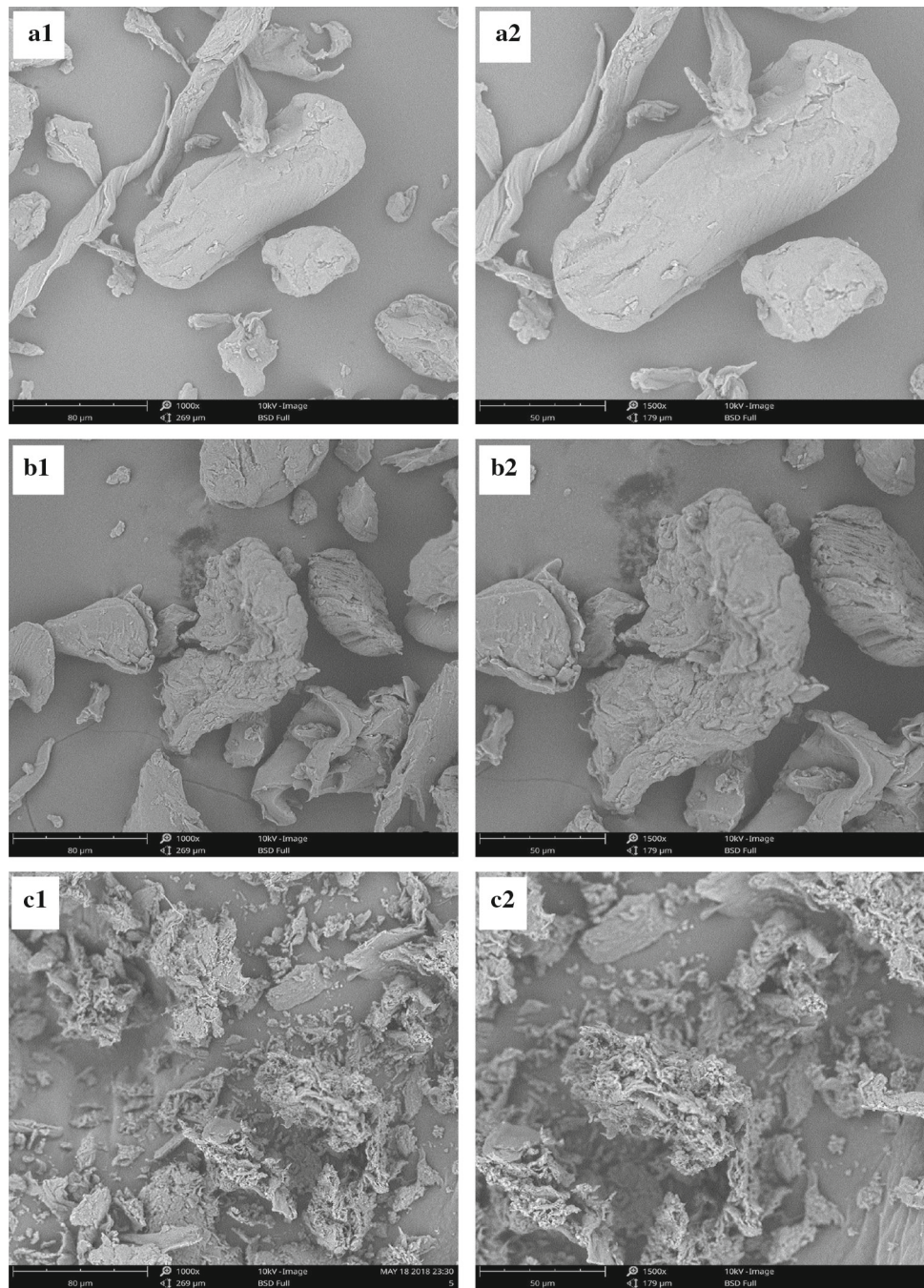


Fig. 6 XRD curves of SG, ESG and MESH

curves are given in Table 4. From Table 4, the esterification and enzymatic hydrolysis decreased the onset decomposition temperature, end decomposition temperature, onset temperature and enthalpy change of ESG and MESH. The enzymatic hydrolysis increased the weight loss rate and peak temperature of ESG, but the esterification reduced the weight loss rate and peak temperature. Therefore, the thermal stability was in order of $\text{MESH} > \text{SG} > \text{ESG}$. It further proved that the enzymatic hydrolysis cut the molecular chains of SG.

Fig. 7 SEM photographs of SG (a), ESG (b) and MESG (c). **a1–c1** SG, ESG and MESG photos magnified 1000 times, respectively. **a2–c2** SG, ESG and MESG photos magnified 1500 times, respectively



3.5 XRD Analysis

The XRD patterns of SG, ESG (DE = 0.175) and MESG (DE = 0.175, DS = 0.812) are shown in Fig. 6. The patterns of SG and ESG were basically same and were composed of peaks at diffraction angles of 11.5°, 14.6°, 17.2°, 20.4° and 23.2°, respectively. The enzymatic hydrolysis only changed the intensity of diffraction peaks. For MESG XRD pattern, the peaks at diffraction angles of 11.5°, 14.6° and 23.2° disappeared, the peaks at 17.2° and 20.4° became weak, and a

new peak arose at 26.6°. It indicated that the crystalline structure of ESG was almost destroyed by the esterification with maleic anhydride. The crystalline degree of SG, ESG and MESG was calculated by MIDI jade 6.0 software as 36.12%, 33.25% and 4.26%, respectively. These evidences proved that the crystalline regions of native SG were basically destroyed by esterification, whereas they were influenced small by the enzymatic hydrolysis.

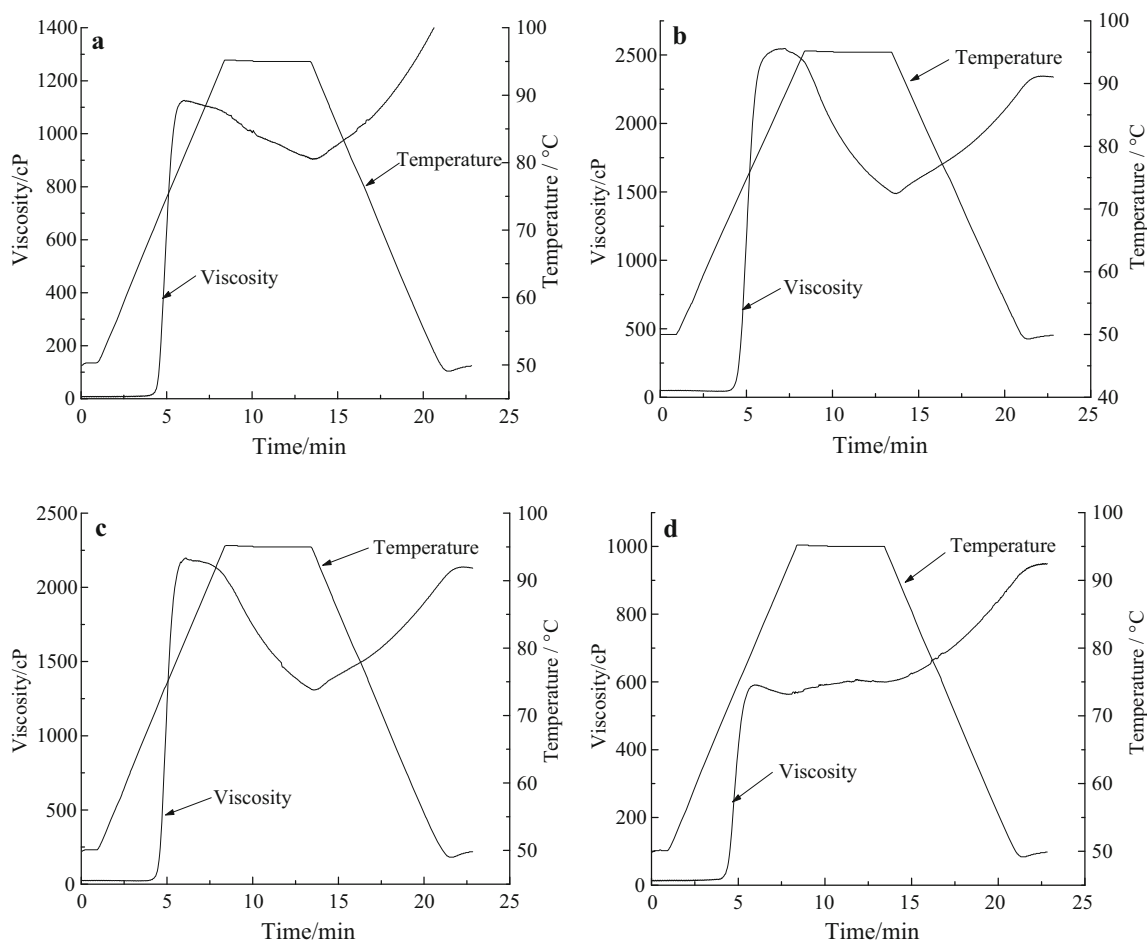


Fig. 8 Effect of adding SG and its derivatives on gelatinization characteristics of potato starch. **a** Potato starch; **b** potato starch added by 0.3% SG; **c** potato starch added by 0.3% ESG; **d** potato starch added by 0.3% MESG

3.6 Particle Morphology

The SEM photographs of SG, ESG (DE = 0.175) and MESG (DE = 0.175, DS = 0.812) are shown in Fig. 7. From Fig. 7, it can be clearly observed that the enzymatic hydrolysis and esterification have greatly changed the appearance of the SG particles. The SG particles exhibited a strip, its surface was smooth, and its size distribution was also uneven. After the enzymatic hydrolysis, the surface of ESG particles became coarse, and many trenches emerged in some of the particles. After further esterification on basis of the enzymatic hydrolysis, the surface of MESG particles became rougher than ESG, and a lot of very deep grooves appeared on MESG particles. It suggested that the structure of SG granules was already severely damaged at this stage. This result was consistent with the preceding result of XRD. At same time, the appearance of many very small grains after the esterification confirmed that the esterification also reduced the intensity of MESG particles due to the destruction.

3.7 Influence of Adding SG and Its Derivatives on Pasting Characteristics of Potato Starch

The effect of adding SG, ESG (DE = 0.175) and MESG (DE = 0.175, DS = 0.812) on pasting characteristics of potato starch is shown in Fig. 8. The amount of adding SG, ESG and MESG was 0.3%, which was referred to as the mass percentage ratio of SG or ESG, MESG to the dry potato starch. From Fig. 8, the pasting characteristics of potato starch were influenced by adding SG and its derivatives. Adding SG could make the peak viscosity of potato starch paste to reach a value of 2458 cP, and adding ESG increased the peak viscosity only to a value of 2198 cP, but the viscosity change trend of the two curves was basically the same. Compared with former two, the gelatinization of potato starch was evidently affected by adding MESG. To further evaluate the effect of adding SG and its derivatives on pasting characteristics of potato starch, the specific characteristic parameters of these curves are listed in Table 5. From Table 5, adding SG and its derivatives affected the pasting temperature, peak viscosity, trough

Table 5 Effect of adding SG, ESG and MESH on gelatinization characteristic parameters of potato starch

Samples	Potato starch	Potato starch added by 0.3% SG	Potato starch added by 0.3% ESG	Potato starch added by 0.3% MESH
Pasting temperature (°C)	71.4	71.9	71.8	70.7
Peak viscosity (cP)	1126.0	2548.0	2198.0	608.0
Trough viscosity (cP)	903.0	1487.0	1308.0	599.0
Final viscosity (cP)	1504.0	2338.0	2129.0	950.0
Setback (cP)	601.0	851.0	821.0	351.0
Breakdown (cP)	223.0	1061.0	890.0	9.0

viscosity, setback and breakdown of potato starch. The peak viscosity, trough viscosity, setback and breakdown of potato starch-added MESH was less than those of potato starch, whereas ones of potato starch-added SG or ESG was greater than those of potato starch, suggesting that ester groups could reduce the pasting characteristics of potato starch, which was different from adding SG or ESG.

4 Conclusions

Through the optimization of response surface, the optimum reaction conditions were as follows: reaction time 80 min, reaction temperature 119 °C, amount of maleic anhydride 40% and amount of ionic liquid 1400%. The factors influencing the esterification of MESH from big to small were reaction temperature, amount of maleic anhydride, amount of ionic liquid and reaction time. The regression model could well evaluate the synthesis of MESH. The peak of stretching vibration of C=O groups at 1718 cm⁻¹ confirmed that the ester groups were successfully grafted to SG molecular chains. The enzymolysis and esterification changed the thermal characteristics of SG. The esterification had great influence on the crystalline regions of native SG, but the enzymatic hydrolysis had small influence on the crystalline regions. Adding MESH evidently reduced the peak viscosity, trough viscosity, final viscosity, setback and breakdown of potato starch and changed the normal shape of gelatinization curve of starch. The successful synthesis of MESH with high DS in ionic liquid will provide more options for the functionalization of many other natural polymers. The effect of adding MESH on the breakdown of potato starch showed that MESH could obviously improve the shearing resistance of starch.

Acknowledgments Authors are grateful to individuals who have supported their research.

Compliance with Ethical Standards

Conflict of interest Authors declare that they have no conflict of interest.

References

- Zhang, L.; Zhang, P.; Li, X.; Cui, Y.: Sesbania gum xanthate supported palladium complex as an efficient catalyst for heck reaction. *J. Appl. Polym. Sci.* **4**, 2198–2202 (2007)
- Rekaby, M.M.; Elthalouth, I.A.; Rahman, A.A.H.; Elkhaby, E.S.: Technological evaluation of carboxymethyl sesbania galactomannan gum, derivatives as thickeners in reactive printing. *BioResources* **5**, 1517–1529 (2010)
- Gallão, M.I.; Furtado, R.S.; de Brito, E.S.: Cytochemical characterization and structural approach to *Prosopis juliflora* (Sw) D.C. seed gum extraction. *J. Sci. Food Agric.* **85**, 2321–2324 (2005)
- Zhang, Q.; Gao, Y.; Zhai, Y.A.; Liu, F.Q.; Gao, G.: Synthesis of sesbania gum supported dithiocarbamate chelating resin and studies on its adsorption performance for metal ions. *Carbohydr. Polym.* **73**, 359–363 (2008)
- Liu, H.J.; Qi, R.L.; Gao, L.; Xue, M.; Shen, D.: Grafting modification of sesbania gum and sizing performance. *Adv. Mater. Res.* **424–425**, 1211–1214 (2012)
- Zhang, Q.; Li, D.; Zhang, H.; Su, G.; Li, G.: Preparation and properties of poly(lactic acid)/sesbania gum/nano-TiO₂ composites. *Polym. Bull.* **75**, 623–635 (2018)
- Pal, P.; Banerjee, A.; Halder, U.; Pandey, J.P.; Sen, G.; Bandyopadhyay, R.: Conferring antibacterial properties on sesbania gum via microwave-assisted graft copolymerization of DADMAC. *J. Polym. Environ.* **26**, 3272–3282 (2018)
- Shen, D.; Xue, M.; Zhang, L.; Liu, H.; Gao, L.; Cui, Y.: Preparation and characterization of oxidized sesbania gum and evaluation of its warp sizing performance for fine cotton yarns. *Polym. Degrad. Stab.* **96**, 2181–2188 (2011)
- Xu, Y.; Miladinov, V.; Hanna, M.A.: Starch acetate-maleate mixed ester synthesis and characterization. *Cereal Chem.* **82**, 336–340 (2005)
- Sarkar, S.; Singhal, R.S.: Esterification of guar gum hydrolysate and gum arabic with n-octenyl succinic anhydride and oleic acid and its evaluation as wall material in microencapsulation. *Carbohydr. Polym.* **86**, 1723–1731 (2011)
- Li, D.; Henschel, J.; Ek, M.: Esterification and hydrolysis of cellulose using oxalic acid dihydrate in a solvent-free reaction suitable for preparation of surface-functionalised cellulose nanocrystals with high yield. *Green Chem.* **19**, 5564–5567 (2017)
- Chi, H.; Xu, K.; Wu, X.; Chen, Q.; Xue, D.; Song, C.; Wang, P.: Effect of acetylation on the properties of corn starch. *Food Chem.* **106**, 923–928 (2008)
- Fonseca-Florido, H.A.; Vázquez-García, H.G.; Méndez-Montealvo, G.; Basilio-Cortés, U.A.; Navarro-Cortés, R.; Rodríguez-Marín, M.L.; Gómez-Aldapa, C.A.: Effect of acid hydrolysis and OSA esterification of waxy cassava starch on emulsifying properties in Pickering-type emulsions. *LWT Food Sci. Technol.* **91**, 258–264 (2018)



14. D'Melo, D.; Sabnis, A.; Shenoy, M.A.; Kathalewar, M.: Preparation of acetylated guar gum—unsaturated polyester composites & effect of water on their properties. *Curr. Chem. Lett.* **1**, 147–156 (2012)
15. Emeje, M.; Kalita, R.; Isimi, C.; Buragohain, A.; Kunle, O.; Ofoefule, S.: Synthesis, physicochemical characterization, and functional properties of an esterified starch from an underutilized source in Nigeria. *Afr. J. Food Agric. Nutr. Dev.* **12**, 7001–7018 (2012)
16. Silaket, P.; Chatakanonda, P.; Tran, T.; Wansuksri, R.; Piyachomkwan, K.; Sriroth, K.: Thermal properties of esterified cassava starches and their maltodextrins in various water systems. *Starch/Stärke* **66**, 1022–1032 (2014)
17. Huang, L.; Xiao, C.; Chen, B.: A novel starch-based adsorbent for removing toxic Hg(II) and Pb(II) ions from aqueous solution. *J. Hazard. Mater.* **192**, 832–836 (2011)
18. Muhammad, K.; Hussin, F.; Man, Y.; Ghazali, H.; Kennedy, J.: Effect of pH on phosphorylation of sago starch. *Carbohydr. Polym.* **42**, 85–90 (2000)
19. Xing, G.X.; Zhang, S.F.; Ju, B.Z.; Yang, J.Z.: Microwave-assisted synthesis of starch maleate by dry method. *Starch/Stärke* **58**, 464–467 (2006)
20. Zuo, Y.; Gu, J.; Yang, L.; Qiao, Z.; Tan, H.; Zhang, Y.: Synthesis and characterization of maleic anhydride esterified corn starch by the dry method. *Int. J. Biol. Macromol.* **62**, 241–247 (2013)
21. Fidale, L.C.; Possidonio, S.; El Seoud, O.A.: Application of 1-allyl-3-(1-butyl)imidazolium chloride in the synthesis of cellulose esters: properties of the ionic liquid, and comparison with other solvents. *Macromol. Biosci.* **9**, 813–821 (2009)
22. Abd El-Thalouth, I.; Reky, M.; Abdel-Rahman, A.H.; El-Khabery, S.A.: Preparation and characterization of phosphorylated sesbania galactomannan gum derivatives and their applications in textile printing. *Res. J. Text. Appar.* **16**, 68–76 (2012)
23. Rossi, B.; Ponzini, E.; Merlini, L.; Grandori, R.; Galante, Y. M.: Characterization of aerogels from chemo-enzymatically oxidized galactomannans as novel polymeric biomaterials. *Eur. Polym. J.* **93**, 347–357 (2017)
24. Li, H.; Gao, L.; Xue, M.; Shen, D.; Cui, Y.: Grafting modification of sesbania gum and its application to textile sizing. *J. Text. Res.* **424**, 1211–1214 (2012)
25. Wang, Z.; Zhu, L.; Zhang, G.; Zhao, G.; Zhu, Y.; Chang, L.: Investigation of pyrolysis kinetics of carboxymethyl hydroxypropyl sesbania gum. *J. Therm. Anal.* **49**, 1509–1512 (1997)
26. Tian, J.; Yin, J.; Tang, X.; Chen, J.; Luo, X.; Rao, G.: Enhanced leaching process of a low-grade weathered crust elution-deposited rare earth ore with carboxymethyl sesbania gum. *Hydrometallurgy* **139**, 124–131 (2013)
27. Tang, H.; Yao, Y.; Li, Y.; Dong, S.: Effect of cross-linking and oxidation on structure and properties of sesbania gum. *Int. J. Biol. Macromol.* **114**, 640–648 (2018)
28. Mudgil, D.; Barak, S.; Khatkar, B.S.: Optimization of enzymatic hydrolysis of guar gum using response surface methodology. *J. Food Sci. Technol.* **51**, 1600–1605 (2012)
29. Endo, R.; Setoyama, M.; Yamamoto, K.; Kadokawa, J.: Acetylation of xanthan gum in ionic liquid. *J. Polym. Environ.* **23**, 199–205 (2014)
30. Tang, H.; Liu, L.; Li, Y.; Dong, S.: Debranching potato starch: synthesis, optimization and thermal property. *Polym. Bull.* **72**, 2537–2552 (2015)
31. Gill, A.N.; Iftikhar, A.; Rashid, A.; Amin, M.; Khan, R.R.M.; Rafique, H.M.; Jelani, S.; Adnan, A.: Lipase-catalyzed green synthesis of starch–maleate monoesters and its characterization. *J. Iran. Chem. Soc.* **15**, 1939–1945 (2018)
32. Pal, P.; Pandey, J.P.; Sen, G.: Grafted sesbania gum: A novel derivative for sugarcane juice clarification. *Int. J. Biol. Macromol.* **114**, 349–356 (2018)
33. Tang, H.; Gao, S.; Li, Y.; Dong, S.: Modification mechanism of sesbania gum, and preparation, property, adsorption of dialdehyde cross-linked sesbania gum. *Carbohydr. Polym.* **149**, 151–162 (2016)
34. Gong, H.H.; Liu, M.Z.; Chen, J.C.; Han, F.; Gao, C.M.; Zhang, B.: Synthesis and characterization of carboxymethyl guar gum and rheological properties of its solutions. *Carbohydr. Polym.* **88**, 1015–1022 (2012)
35. Sujka, M.; Jamroz, J.: Ultrasound-treated starch: SEM and TEM imaging, and functional behaviour. *Food Hydrocolloids* **31**, 413–419 (2013)
36. Raquez, J.-M.; Nabar, Y.; Srinivasan, M.; Shin, B.-Y.; Narayan, R.; Dubois, P.: Maleated thermoplastic starch by reactive extrusion. *Carbohydr. Polym.* **74**, 159–169 (2008)
37. Verma, S.; Ahuja, M.: Carboxymethyl sesbania gum: Synthesis, characterization and evaluation for drug delivery. *Int. J. Biol. Macromol.* **98**, 75–83 (2017)
38. Zhou, H.; Wang, J.; Li, J.; Fang, X.; Sun, Y.: Pasting properties of *Angelica dahurica* starches in the presence of NaCl, Na₂CO₃, NaOH, glucose, fructose and sucrose. *Starch/Stärke* **63**, 323–332 (2011)
39. Lan, S.; Leng, Z.; Guo, N.; Wu, X.; Gan, S.: Sesbania gum-based magnetic carbonaceous nanocomposites: facile fabrication and adsorption behavior. *Colloids Surf. A* **446**, 163–171 (2014)
40. Zuo, Y.; Gu, J.; Yang, L.; Qiao, Z.; Tan, H.; Zhang, Y.: Preparation and characterization of dry method esterified starch/poly(lactic acid) composite materials. *Int. J. Biol. Macromol.* **64**, 174–180 (2014)